Frontiers in Bioscience Landmark

Front. Biosci. (Landmark Ed) **2023**; 28(12): 339
https://doi.org/10.31083/j.fbl2812339

Original Research

Transcriptome-Wide Dynamics of m7G-Related LncRNAs during the Progression from HBV Infection to Hepatocellular Carcinoma

Min Shi[1,†], Shunshun Zhu[1,†], Linying Sun[2,†], Jieli Hu[3], Hao Li[4], Wenqing Dai[5], Ning Song[6], Minmin Li[6], Ying Wu[7], Donghua Xu[5,*], Tao Guo[1,*]

[1]Department of Pathophysiology, School of Basic Medical Sciences, Weifang Medical University, 261053 Weifang, Shandong, China
[2]Department of Functional Laboratory, School of Basic Medical Sciences, Weifang Medical University, 261053 Weifang, Shandong, China
[3]Key Laboratory of Molecular Biology on Infectious Diseases, Ministry of Education, Chongqing Medical University, 400016 Chongqing, China
[4]Hepatobiliary and Pancreatic Medicine Center, The First Affiliated Hospital of Weifang Medical University, 261000 Weifang, Shandong, China
[5]Central Laboratory, The First Affiliated Hospital of Weifang Medical University, 261000 Weifang, Shandong, China
[6]School of Stomatology, Weifang Medical University, 261053 Weifang, Shandong, China
[7]Liuzhou Key Laboratory of Infection Disease and Immunology, Guangxi Health Commission Key Laboratory of Clinical Biotechnology, Liuzhou People's Hospital Affiliated to Guangxi Medical University, 545006 Liuzhou, Guangxi, China
*Correspondence: xudh@wfmc.edu.cn (Donghua Xu); guotao@wfmc.edu.cn (Tao Guo)
[†]These authors contributed equally.

Academic Editor: Marco Falasca
Submitted: 21 July 2023 Revised: 18 September 2023 Accepted: 21 September 2023 Published: 19 December 2023

Abstract

Background: The functional ramifications of internal N7-methylguanosine (m7G) modification on RNAs have recently come to light, yet its regulatory influence on long noncoding RNAs (lncRNAs) during the inflammatory-carcinogenesis transformation process in hepatitis B virus (HBV)-mediated hepatocellular carcinoma (HCC) remains largely unexplored. **Methods**: Clinical surgical samples encompassing HBV-related HCC, comprising both HCC tissue (tumor group, HBV+) and corresponding adjacent liver tissue (paracancerous group, HBV+), were collected for analysis. Additional adjacent normal liver tissues (normal group, HBV-) were acquired from patients with hepatic hemangioma, serving as controls. Employing MeRIP-seq, differential m7G levels of lncRNAs across these groups were compared to identify a subset of lncRNAs exhibiting continuous and dynamic changes in m7G modification. Subsequently, *in vitro* validation was conducted. **Results**: A total of 856 lncRNAs exhibited alterations in m7G modification when compared to paracancerous tissue and normal tissue. Similarly, 1775 lncRNAs displayed changes in m7G modification when comparing HCC tissue to paracancerous tissue. For intergroup comparison, orthogonal analysis revealed that 6 lncRNAs consistently demonstrated hyper-m7G modification. *In vitro* validation confirmed that among these 6 lncRNAs, TEKT4P2 and DNM1P41 exhibited m7G modification-dependent expression. **Conclusions**: This study provides a comprehensive analysis of lncRNA m7G modification during the inflammatory-carcinogenesis transformation process in HBV-mediated HCC. The findings highlight the potential for multiple lncRNAs to undergo m7G modification changes, with TEKT4P2 and DNM1P41 identified as promising molecular targets within this intricate regulatory landscape.

Keywords: HBV-related HCC; lncRNA; m7G

1. Introduction

Primary hepatic carcinoma, one of the prevalent neoplasms in humans, currently ranks as the third leading cause of cancer-related mortality [1]. The majority of primary hepatic carcinomas comprise hepatocellular carcinoma (HCC) [2]. HCC development can be instigated by a multitude of factors, including dietary aspects, metabolic conditions, microbial infections, and environmental exposures, among others [3]. Despite advancements in clinical practice, early diagnosis and intervention of HCC remain formidable challenges. Moreover, the limited curability and high recurrence rates associated with HCC remain unresolved issues [4].

Hepatitis B virus (HBV) is a major etiological factor in the development of HCC [5] and has emerged as a prominent cause, particularly in developing countries, with a notable prevalence in the Asian region [6]. Prolonged HBV infection leads to liver damage, triggering sequential progression from chronic hepatitis B to liver fibrosis and ultimately culminating in HCC [7]. Typically, the clinical course of chronic HBV infection follows a characteristic trajectory encompassing inflammation, liver cirrhosis, and subsequent formation of HCC, which may span several years at each stage [8]. However, it is noteworthy that HBV infection can lead directly to HCC without the presence of liver cirrhosis [9]. Regardless of the tissue phenotype, the occurrence and development of HBV-mediated HCC involve a diverse array of molecular imbalances characterized by genetic and epigenetic alterations, including point mutations, chromosomal aberrations, and epigenetic modifications, which are considered pivotal pathways in this context [10].

With the advancement of sequencing technologies, long noncoding RNAs (lncRNAs) have gradually gained

recognition and been proven to be closely associated with the occurrence and development of HCC [11,12]. Additionally, lncRNAs have been shown to play an important role in HBV-related HCC by interacting with HBV [13,14]. Concurrently, internal modifications of RNA, especially methylation, have attracted considerable attention in recent years [15]. The common mRNA 5′ end modification N7-methylguanosine (m7G) is also an internal modification of noncoding RNA and has a crucial impact on RNA processing, cellular localization, and functional activities, regulating the stability and expression levels of RNA. This has significant importance on RNA expression and its regulatory role in tumors [16]. However, reports investigating the influence of internal m7G modification on lncRNA expression and function are currently limited. In this study, our objective was to use clinical tissues and m7G-sequencing technology to elucidate the dynamic alterations occurring in lncRNA m7G modification throughout the continuum from HBV infection to HBV-related HCC. Additionally, we aimed to identify lncRNAs that undergo dynamic changes facilitated by m7G modification, encompassing comprehensive profiling from the inflammatory processes to the initiation of hepatocarcinogenesis.

2. Methods

2.1 Clinical Sample and Ethics Application

Clinical specimens were acquired from 6 patients who underwent hepatic resection at the First Affiliated Hospital of Weifang Medical University. The cohort comprised 3 patients with HBV-negative hepatic hemangioma (HHE) and 3 patients with HBV-related HCC (positive HBsAg, serum HBV DNA >500 IU/mL). All enrolled patients signed informed consent forms, and ethical clearance for this study was obtained from the institutional ethics committee. Strict exclusion criteria were applied prior to patient enrollment, as follows: (1) history of malignancy or concurrent multiple tumors; (2) substantiated evidence of alcohol abuse or a background of nonalcoholic steatohepatitis (NASH); (3) intrahepatic malignancies other than HCC; and (4) previous administration of chemotherapy or local transcatheter arterial chemoembolization (TACE) treatment before surgical intervention. Ultimately, three patients with HBV-related HCC were included in this investigation, with their respective tumor tissues and adjacent liver tissues classified as the HBV-positive tumor group and the HBV-positive liver group (paracancerous group), respectively. Additionally, three patients with HBV-negative hepatic hemangioma were included, and adjacent normal liver tissues were used as the normal group (**Supplementary Table 1**). Thus, a total of 9 specimens obtained from 6 patients were categorized into 3 groups for comparison (Fig. 1). To investigate the association between HBV and the m7G modification of lncRNAs, comparative analysis was conducted specifically focusing on the paracancerous group and the normal group. Simultaneously, comparison was made between the tumor group and the paracancerous group to assess the plausible correlation between tumorigenesis and anomalous m7G modification of lncRNAs.

2.2 Cell Culture and Transfection

Cell culture was conducted using complete medium comprising DMEM (SH30022.01B, HyClone, Logan, UT, USA) supplemented with 10% fetal bovine serum (S711-001S, Lonsera, Ciudad de la Costa, Carnelones, Uruguay). Normal liver L02 cells and HBV-related hepatoma Hep3B2.1-7 cells were sourced from Duolaimi Biotechnology (Wuhan, Hubei, China) and Pricella Cell Bank (Procell Life Science & Technology Co., Ltd. Wuhan, Hubei, China), respectively. The normal hepatocyte cell line WRL68 and HBV-related hepatoma HepG2.2.15 cells were purchased from Fenghui Biotechnology (Changsha, Hunan, China). All cell lines were validated by STR profiling and tested negative for mycoplasma. Cells were all cultured in a humidified incubator at 37 °C and 5% CO_2. pcDNA3.1 plasmids expressing METTL1 and WDR4 and their small interfering RNAs (siRNAs) were synthesized by Duolaimi Biotechnology (Wuhan, Hubei, China). The pCH-9/3091 plasmid, which contains an HBV 1.1× genome controlled by the CMV-IE promoter [17], was utilized for HBV transfection. Transfection was carried out using Lipofectamine 2000 (11668019, Thermo Fisher, Waltham, MA, USA) following the manufacturer's instructions.

2.3 Enzyme Linked Immunosorbent Assay (ELISA)

After transfecting L02 cells and WRL68 cells with HBV for 72 hours, the cell culture supernatant was collected for analysis. The presence of hepatitis B e antigen (HBeAg) and hepatitis B surface antigen (HBsAg) was determined using diagnostic ELISA kits (202301012 and 202212402, KHB, Shanghai, China) in accordance with the manufacturer's instructions. To detect HBsAg, 75 µL of the cell culture supernatant sample was added to each well of a reaction plate and incubated at 37 °C for 60 minutes. Subsequently, 50 µL of enzyme conjugate was added to the positive and negative control wells. The plate was gently shaken for 10 seconds and then incubated at 37 °C for 30 minutes. Following a wash step with wash buffer, a chromogenic substrate was added, and the plate was incubated at 37 °C for 30 minutes. The cut-off value (COV) for HBsAg detection was determined as the average optical density (OD) of the negative control plus 0.1. For HBeAg detection, 50 µL of the cell culture supernatant sample was added to each well of the reaction plate and incubated at 37 °C for 30 minutes. After washing, a chromogenic substrate was added, and the plate was incubated at 37 °C for 15 minutes. Finally, optical density (OD) values were measured at 450 nm. The COV for HBeAg was calculated as either 0.05 (if OD <0.05) × 2.1, or the measured OD (if OD ≥ 0.05) × 2.1. Samples with OD values greater than the COV were considered positive for HBeAg and HBsAg.

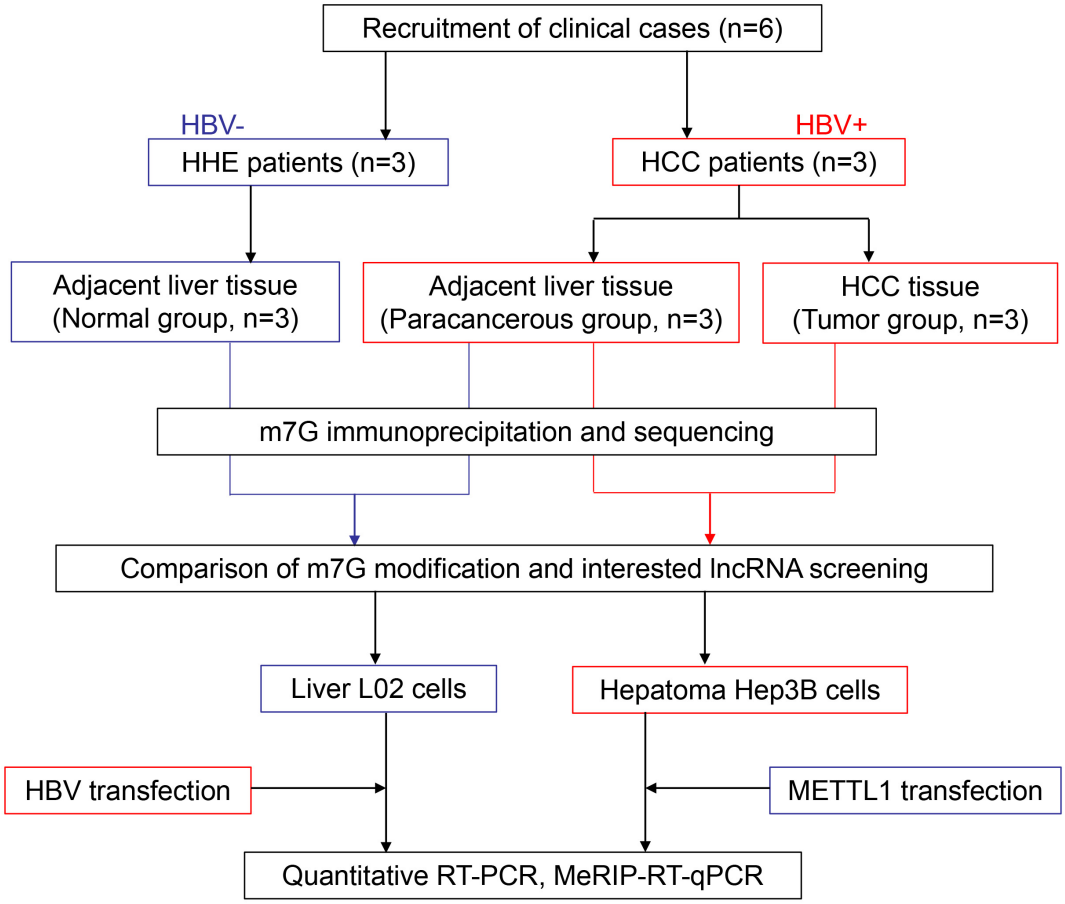

Fig. 1. Flow chart for inclusion and analysis of clinical tissues. HBV, Hepatitis B virus; HHE, hepatic hemangioma; HCC, hepatocellular carcinoma; lncRNAs, long noncoding RNAs; RT-PCR, reverse transcription-PCR; MeRIP-RT-qPCR, methylated RNA immunoprecipitation-reverse transcription-PCR.

2.4 Quantitative Reverse Transcription-PCR (qRT–PCR)

RNA extraction was carried out using RNA Rapid Extraction Kit (220011, Fastagen, Shanghai, China) following established protocols. The concentration of total RNA was determined using a NanoDrop2000 instrument (N50, Implen, LA, USA), and samples with an A260/A280 ratio $\geq$1.8 were deemed suitable for downstream analyses. Reverse transcription (RT) was performed using ReverTra Ace qPCR RT Kit (FSQ-101, Toyobo-Shanghai, Shanghai, China) at 37 °C for 15 minutes. Subsequently, quantitative PCR was conducted using the Prism® 7900HT instrument (ABI, Carlsbad, CA, USA) with SYBR® Premix (QPK-212, Toyobo-Shanghai, Shanghai, China), specific primers (**Supplementary Table 2**), and ddH_2O. β-Actin was selected as the internal reference, and quantitative comparisons were obtained using the $2^{-\Delta\Delta Ct}$ calculation method.

2.5 MeRIP-Seq

Total RNA underwent decapping using an RNA decapping enzyme (M0608S, New England Biolabs, Ipswich, MA, USA) and was subsequently immunoprecipitated using GenSeq® Low Input Whole RNA Library Prep Kit (GS-ET-004, GenSeq, Shanghai, China) following the manufacturer's instructions. In brief, RNA was randomly fragmented to approximately 200 nt using the RNA fragmentation reagents provided in the kit; the m7G antibody was coupled to Protein A/G beads by rotating at room temperature for 1 hour. The RNA fragments were then incubated with bead-linked antibodies and rotated at 4 °C for 4 hours. After the incubation period, the RNA/antibody complexes underwent washing, and the captured RNA was eluted from the complexes and purified. The libraries were validated using an Agilent 2100 Bioanalyzer (2100, Agilent, Santa Clara, CA, USA) before being sequenced using the NovaSeq platform (Illumina 6000, Illumina-China, Shanghai, China). The m7G-Seq service was provided by CloudSeq Inc. (Shanghai, China).

Post sequencing, MACS software (v1.4.2, Baylor College of Medicine, Houston, TX, USA) [18] was employed to identify methylation sites (peaks) on RNA. Subsequently, diffReps software (v1.55.6, Shen Lab at Mount Sinai, NY, USA) was used to identify and normalize differentially methylated sites based on peak calling with a fold change (FC) >2 (or <0.05) and $p < 0.00001$ [19].

Genes of interest were visualized using Integrative Genomics Viewer (IGV) software (v2.4.10, Broad Institute, Berkeley, CA, USA) [20]. Gene Ontology (GO) and Kyoto Encyclopedia of Genes and Genomes (KEGG) enrichment analyses were performed separately on associated protein-coding genes with differentially m7G methylated peaks derived from lncRNA transcripts. Additionally, sequence motifs associated with m7G were identified within each group [21]. Orthogonal analysis of hyper- or hypo-m7G between HBV+ vs. HBV- and paracancerous vs. tumor samples was conducted to identify potential m7G-related lncRNAs.

2.6 MeRIP-RT–qPCR

Cells were separately transfected with the HBV-1.1 plasmid and overexpressed/knockdown METTL1 and WDR4, followed by total RNA extraction and m7G immunoprecipitation as described above. After RNA immunoprecipitation, differential peaks related to m7G were identified as potential modification regions for each respective gene. Subsequently, we utilized different primers (**Supplementary Table 2**) in quantitative RT–PCR to compare differential expression of peak-associated fragments between groups, confirming changes in m7G levels.

2.7 Statistical Analyses

Data from three or more independent experiments are presented as the mean ± standard deviation (SD). Statistical analysis was performed using Student's *t* test, and a *p* value of <0.05 was considered statistically significant. The data were processed and presented using GraphPad Prism software (v9.3, GraphPad Software, San Diego, CA, USA).

3. Results

3.1 Overview of m7G Methylation in the Included Samples

The 9 clinical samples obtained from 6 patients were categorized into three groups, as described in Fig. 1. Raw m7G sequencing data were subsequently uploaded to the Gene Expression Omnibus (GEO) database (GSE237003). After summarizing the peaks in each group and conducting intersection analysis, we found that only 97 peaks were shared among all tissues (Fig. 2A). However, corresponding to these peaks, there were 3797 lncRNAs that exhibited the potential for m7G modification across all three groups (Fig. 2B). This indicates the potential presence of multiple peaks available for m7G modifications across different lncRNAs. Furthermore, a consistent overall chromosomal origin of the peaks and lncRNAs was observed (Fig. 2C,D), with lncRNAs primarily being derived from exon sense overlapping regions and intergenic gene regions in all tissues (Fig. 2E). Based on the peak sequences, motif analysis unveiled partially coherent clusters of motifs among the groups. This points toward potential shared enrichment of m7G modification sequences across the different groups (Fig. 2F).

3.2 The Distribution Pattern of Differentially Methylated lncRNAs

To investigate variations in m7G methylation among different lncRNA samples, comparative analysis of internal m7G modifications was initially conducted. Compared to the normal group, 856 lncRNAs underwent m7G modification in the paracancerous group, with 76.1% exhibiting hypermethylation (hyper-m7G) and only 23.9% displaying hypomethylation (hypo-m7G) (Fig. 3A). The majority of these m7G-modified lncRNAs originated from exon sense overlapping regions and intergenic regions (Fig. 3B). We observed the same pattern in comparison between the tumor group and the paracancerous group (Fig. 3C,D). This suggests that during progression from HBV infection to HCC, lncRNAs primarily undergo hyper-m7G. Moreover, the chromosomal origin distribution of the differentially m7G-modified lncRNAs was generally consistent with that of the lncRNAs with m7G-related peaks in different tissues (Fig. 3E,F). Interestingly, shorter lncRNAs exhibited a higher frequency of internal m7G modification changes across all groups, regardless of hyper- or hypo-m7G methylation (Fig. 3G,H). This suggests a greater propensity for m7G methylations to occur within shorter lncRNAs.

3.3 Functional Analysis of Genes Associated with Differentially m7G-Modified lncRNAs

We subsequently conducted functional analysis based on the relationship between m7G methylated peaks and the associated functional genes involved via GO and KEGG analyses. When comparing with the normal group, we observed distinct occurrences of hyper-m7G in 689 peaks sourced from different genes in the paracancerous tissue group, whereas 211 peaks displayed hypo-m7G (Fig. 4A). GO and KEGG analyses were then performed using the associated genes of these aberrant peaks. The results revealed that the genes associated with hyper-m7G peaks were enriched in multiple pathways (Fig. 4B–E, **Supplementary Fig. 1A–D**). Notably, the analysis suggested a potential correlation between the enriched genes and regulation of the Notch pathway (Fig. 4C,E, **Supplementary Fig. 1A,D**). Multiple pathways were also enriched among the genes associated with hypo-m7G peaks. However, cross-analysis of GO and KEGG did not reveal significant functional pathway convergence (Fig. 4F–I, **Supplementary Fig. 1E–H**). In subsequent analysis, we compared the HCC group to the paracancerous group. Relative to the paracancerous tissue, the HCC tissue displayed 1086 hyper-m7G peaks and 799 hypo-m7G peaks (Fig. 5A). GO and KEGG analyses revealed that genes associated with both hyper-m7G peaks (Fig. 5B–E, **Supplementary Fig. 2A–D**) and hypo-m7G peaks were enriched in multiple pathways (Fig. 5F–I, **Supplementary Fig. 2E–H**), including those associated with cancer regulation (Fig. 5E, **Supplementary Fig. 2D,H**).

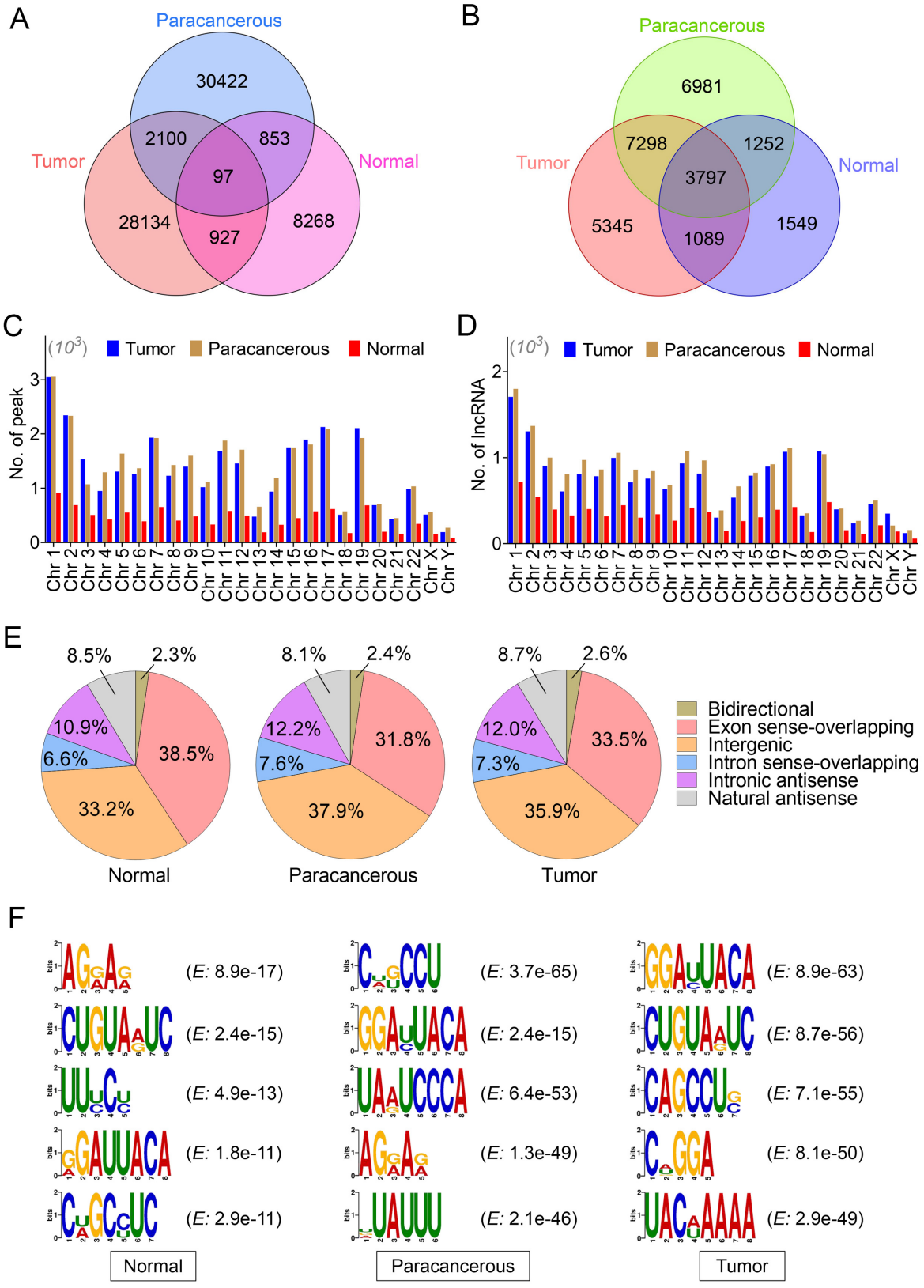

Fig. 2. The N7-methylguanosine (m7G) modification landscape of lncRNAs within clinical samples. Venn diagrams present (A) detected m7G peaks and (B) matched lncRNAs in different tissues. The distribution of (C) m7G peaks and (D) matched lncRNAs in chromosomal origins. (E) Pie charts depict categorized sources of the detected lncRNAs across various clinical specimens. (F) The top 5 enriched motifs enriched in m7G peaks identified from different clinical tissues.

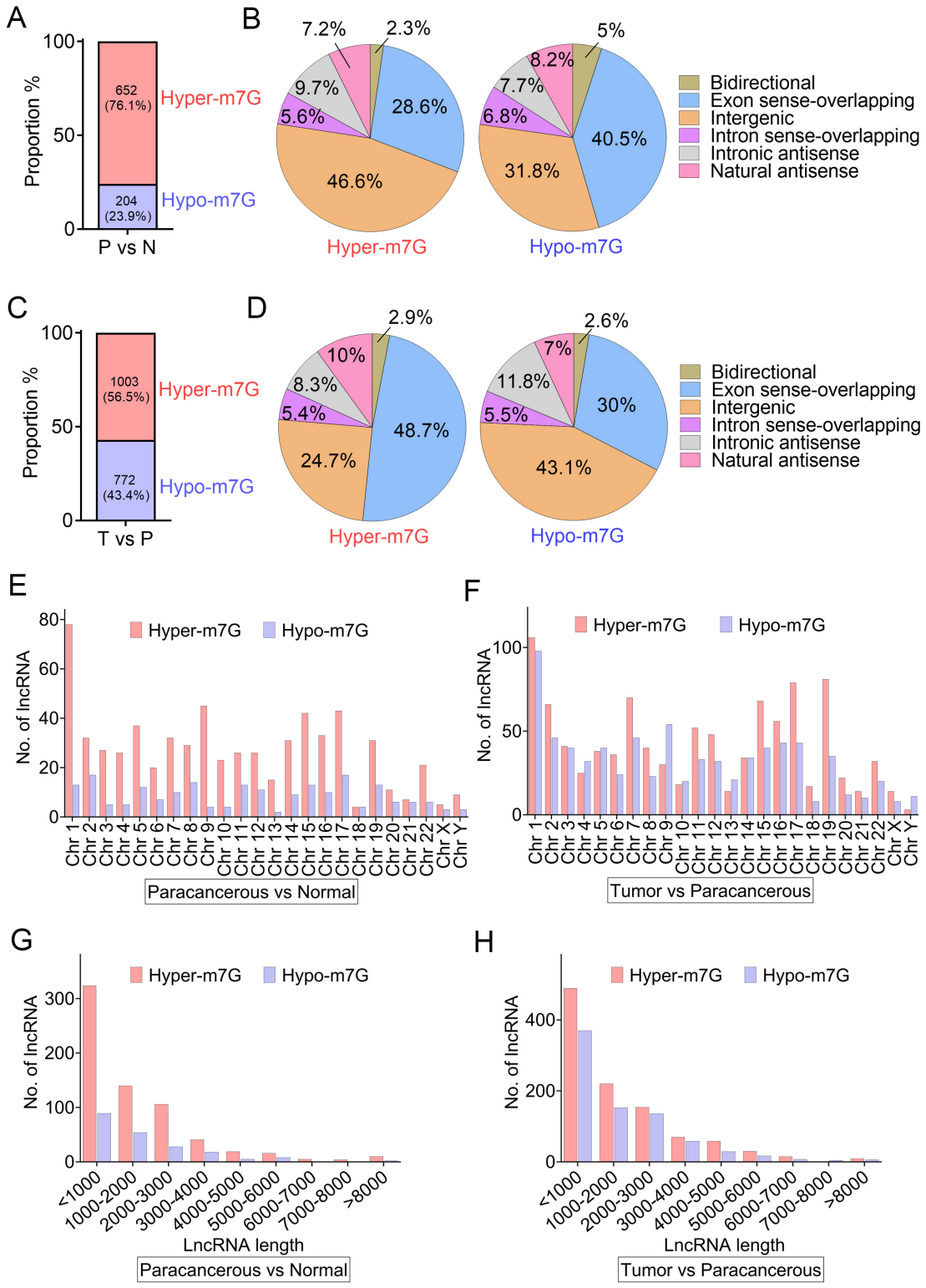

Fig. 3. Differential analysis of m7G modifications of lncRNAs across clinical tissues. (A) The distribution and (B) categorization of lncRNAs exhibiting m7G hypermethylation (hyper-m7G) and hypomethylation (hypo-m7G) compared between the paracancerous group and the normal group. (C) The distribution and (D) classification of lncRNAs with alternative m7G modifications compared between the tumor group and paracancerous group. (E) Chromosomal origins of lncRNAs with hyper-m7G and hypo-m7G compared between the paracancerous group and the normal group. (F) Chromosomal origins of lncRNAs with aberrant m7G modification compared between HCC tissue and paracancerous tissue. The length summary of lncRNAs with aberrant m7G modification (G) compared between the paracancerous group and normal group, as well as (H) between HCC tissue and paracancerous tissue; N, normal; P, paracancerous; T, tumor.

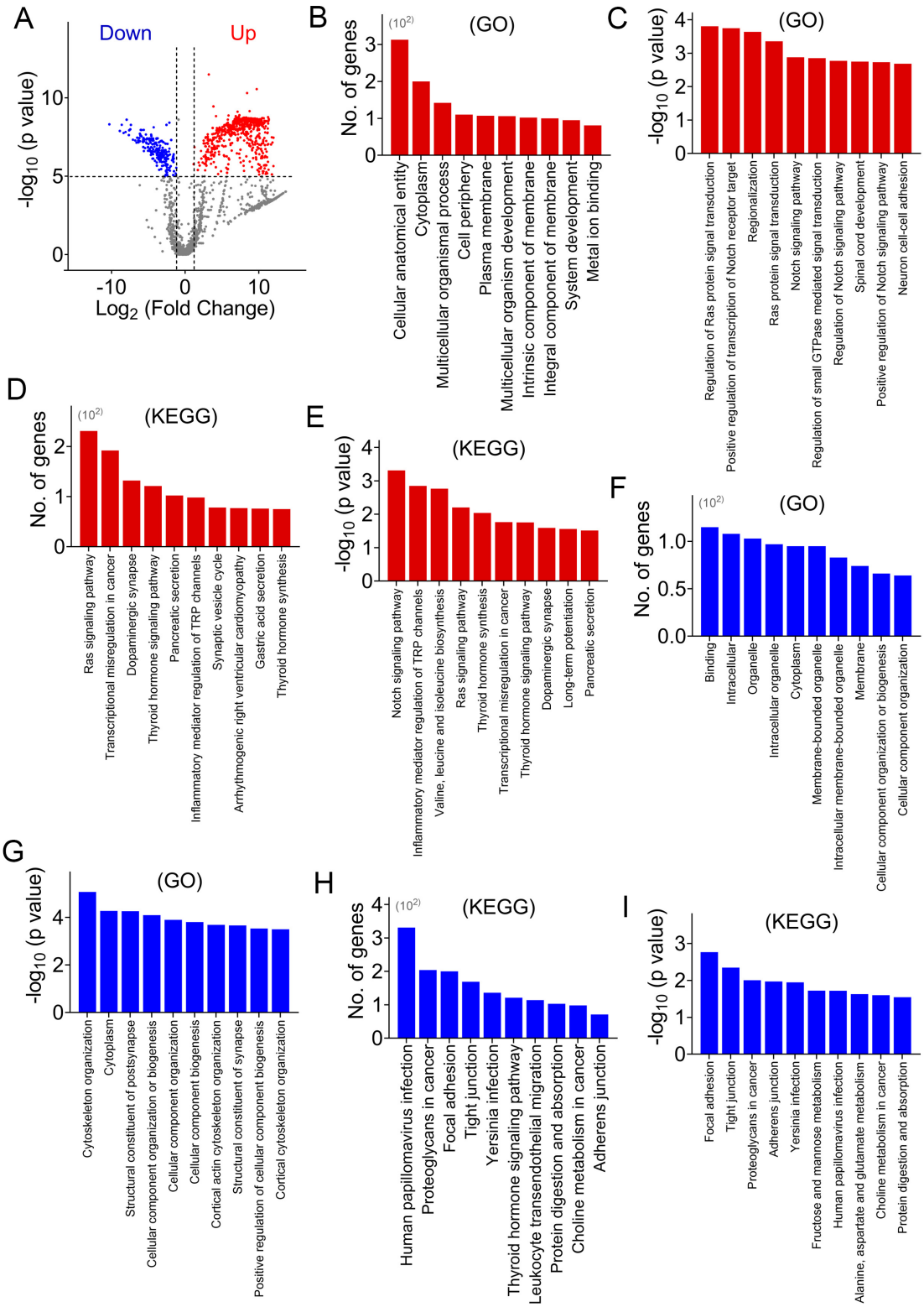

Fig. 4. Functional analysis of associated functional genes of differentially methylated lncRNAs in paracancerous tissue compared to normal liver tissue. (A) The volcano plot displays the peaks of lncRNAs undergoing m7G methylation changes. For genes associated with hyper-m7G peaks, the top 10 terms of GO analysis according to (B) enriched gene count and (C) differential significance, as well as the top 10 KEGG pathways regarding (D) enriched gene count and (E) differential significance, are summarized. For genes associated with hypo-m7G peaks, the top 10 GO analysis terms based on (F) enriched gene count and (G) lowest *p* value, as well as the top 10 KEGG pathways regarding (H) enriched gene count and (I) lowest *p* value, are summarized. GO, Gene Ontology; KEGG, Kyoto Encyclopedia of Genes and Genomes.

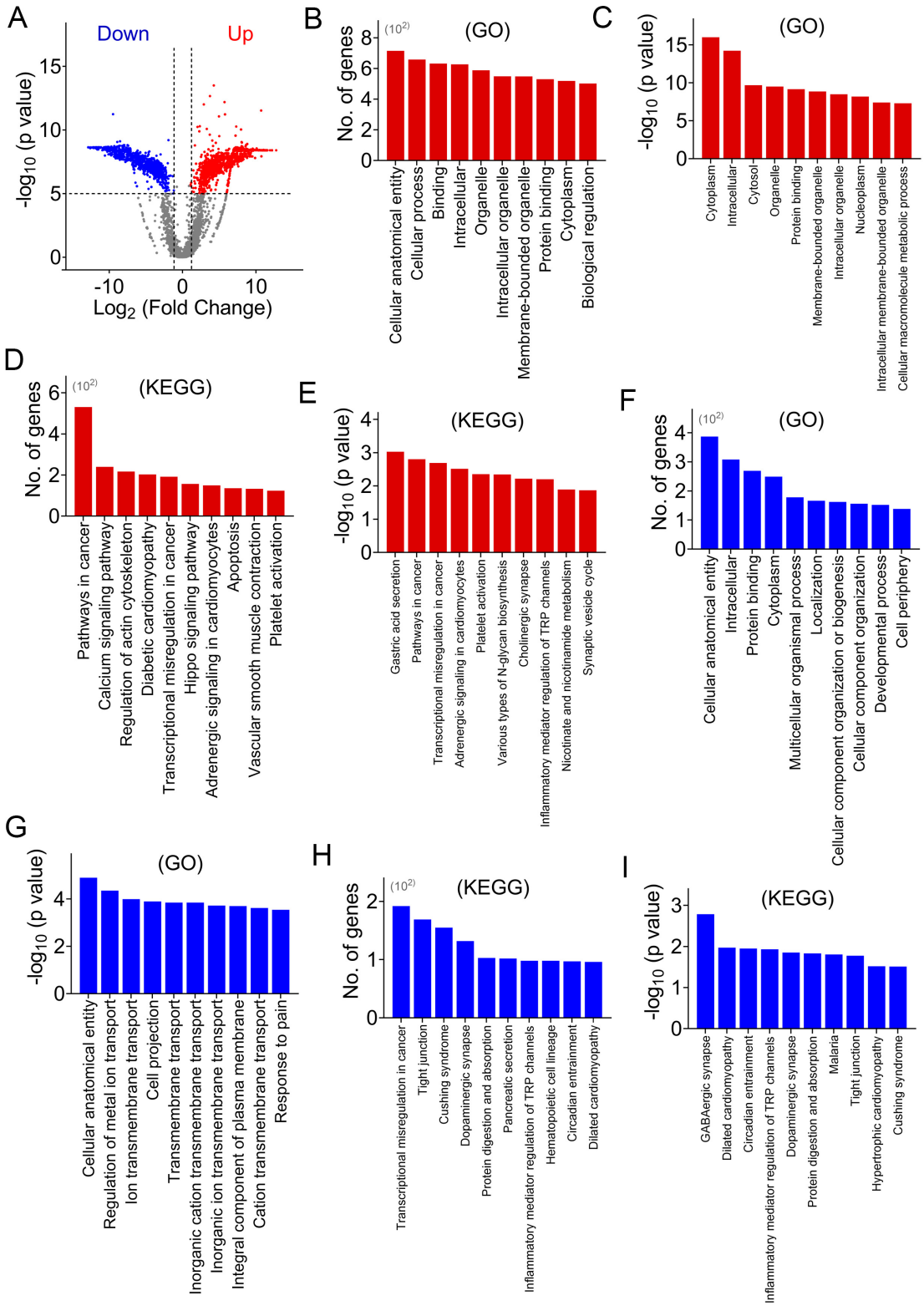

Fig. 5. Functional analysis of associated genes of differentially methylated lncRNAs in HCC tissue compared to paracancerous tissue. (A) The volcano plot presents the peaks of lncRNAs with alternative m7G modification. For hyper-m7G-associated genes, the top 10 enriched GO analysis terms are summarized based on (B) the number of enriched genes and (C) the extent of differential expression. Similarly, the top 10 enriched KEGG pathways are summarized based on (D) the number of enriched genes and (E) the extent of differential expression. For hypo-m7G-associated genes, the top 10 enriched terms of GO analysis are summarized according to (F) the enriched gene count and (G) the differential significance. Similarly, the top 10 enriched KEGG pathways are summarized regarding (H) the enriched gene count and (I) the lowest *p* value.

3.4 Identification of m7G-Associated lncRNAs as Dynamic Markers

To identify lncRNAs with dynamic m7G modifications from HBV infection to hepatocarcinogenesis, we conducted comprehensive screening based on the extent of m7G alterations across different tissues using a FC threshold of >100 or <0.01. It was observed that 470 peaks displayed hyper-m7G and 13 peaks showed hypo-m7G modifications in paracancerous tissue compared to normal liver tissue (Fig. 6A); 352 peaks exhibited FC >100 and 338 peaks had FC <0.01 in comparison between the HCC group and the paracancerous group (Fig. 6B). We then matched these peaks with their corresponding lncRNAs and discovered similar proportional changes, and the top 10 FCs of m7G modifications in different group comparisons are presented in **Supplementary Tables 3,4**. Further intersection analysis revealed that under these screening criteria, 6 lncRNAs (RP11-640N11.2, TEKT4P2, PARP1P1-201, DPP6-210, RP11-989E6.11, DNM1P41) consistently exhibited significant hyper-m7G across intergroup comparisons (Fig. 6C,D). Moreover, we demonstrated the presence of these 6 lncRNAs by visualizing the peaks with significant m7G alterations (Fig. 6E). Therefore, these 6 lncRNAs may serve as potential, dynamically evolving molecular markers during the process from HBV infection to tumorigenesis.

3.5 Validation of the m7G Modification of the Screened lncRNAs

To further substantiate the identified 6 m7G-related lncRNAs with dynamic alterations, we transfected the HBV 1.1 plasmid into normal liver L02 cells and WRL68 cells (**Supplementary Fig. 3A,B**) and subsequently evaluated expression levels of the 6 selected lncRNAs. The results showed significant upregulation exclusively in TEKT4P2 and DNM1P41, but the remaining 4 lncRNAs exhibited no significant changes in expression (Fig. 7A,B). Moreover, HBV transfection led to an increase in m7G levels in both TEKT4P2 and DNM1P41 (Fig. 7C,D). We then investigated alteration of the m7G methyltransferases METTL1 and WDR4 after HBV transfection. The findings revealed significant upregulation of METTL1 and WDR4 in response to HBV in both L02 and WRL68 cells (Fig. 7E,F). Therefore, we hypothesize that expression levels of TEKT4P2 and DNM1P41 are regulated by HBV-mediated m7G modifications. To test our hypothesis, we overexpressed METTL1 and WDR4 in L02 and WRL68 cells (**Supplementary Fig. 3C,D**) and observed significant upregulation of TEKT4P2 and DNM1P41 expression levels (Fig. 8A,B). In addition, we overexpressed METTL1 and WDR4 in HBV-related hepatoma cells (**Supplementary Fig. 3E,F**), Hep3B2.1-7 and HepG2.2.15 cells and found upregulation of TEKT4P2 and DNM1P41 (Fig. 8C,D). To ascertain the association between this upregulation and m7G modification, we overexpressed METTL1 and WDR4 in the aforementioned cells and assessed changes in m7G modifications of TEKT4P2 and DNM1P41. The results indicated that the m7G levels of TEKT4P2 and DNM1P41 were indeed influenced by regulation of METTL1 and WDR4, thereby affecting their own expression levels (Fig. 8E–H). Finally, to confirm the significant regulatory roles of HBV and m7G methyltransferases on TEKT4P2 and DNM1P41, we initially examined differences in m7G modifications of TEKT4P2 and DNM1P41 among different cell lines. The results showed that the m7G levels of TEKT4P2 and DNM1P41 were significantly higher in hepatoma cells than in normal hepatocytes (Fig. 9A,B). We thus transfected HBV 1.1 into L02 and WRL68 cells while simultaneously knocking down m7G methyltransferases (METTL1 or WDR4) (**Supplementary Fig. 3G,H**). The results demonstrated that both HBV and m7G methyltransferases have remarkable impacts on TEKT4P2 and DNM1P41 m7G modification (Fig. 9C–F).

4. Discussion

To date, more than 150 distinct RNA modifications have been identified, with the most prevalent being N6-methyladenosine (m6A), 5-methylcytosine (m5C), N1-methyladenosine (m1A), 3-methylcytidine (m3C), and N7-methylguanosine (m7G) [22]. The m7G modification, referring to methylation at the seventh nitrogen position on RNA guanylate, is commonly observed in mRNA, rRNA, tRNA, and miRNA [23–25]. Similar to other epigenetic modifications, m7G modification is dynamically regulated by RNA methyltransferases and proteins involved in m7G recognition. In the context of cancer regulation, the focus of research has predominantly been on m7G-modified tRNA and miRNA [26,27], with limited studies exploring the impact of m7G modification on long noncoding RNA (lncRNA) functionality. Additionally, there is currently no documented research on the influence of HBV on m7G modification or the dynamic changes in m7G modification during progression of HBV-related HCC.

Our findings reveal that the majority of localized peaks exhibit tissue specificity but that a significant portion of matched lncRNAs are shared across diverse tissues. This highlights the prevalence of m7G-modified lncRNAs that are common between tissues, though there may be variations in the modified sites within each tissue. Moreover, we observed a consistent distribution of peaks and matched lncRNAs on chromosomes, and the proportions of the identified lncRNA sources were similar across different tissues. This suggests that m7G modification sites are widely distributed and closely associated with lncRNAs. Notably, we also discovered enrichment of shared motifs in different tissues, indicating the presence of conserved m7G modification sites or intricate relationships between m7G-related lncRNAs that may play a role throughout progression from HBV infection to HCC. Based on intergroup differential analysis, hyper-m7G predominates during progression from HBV infection to HCC occurrence. This

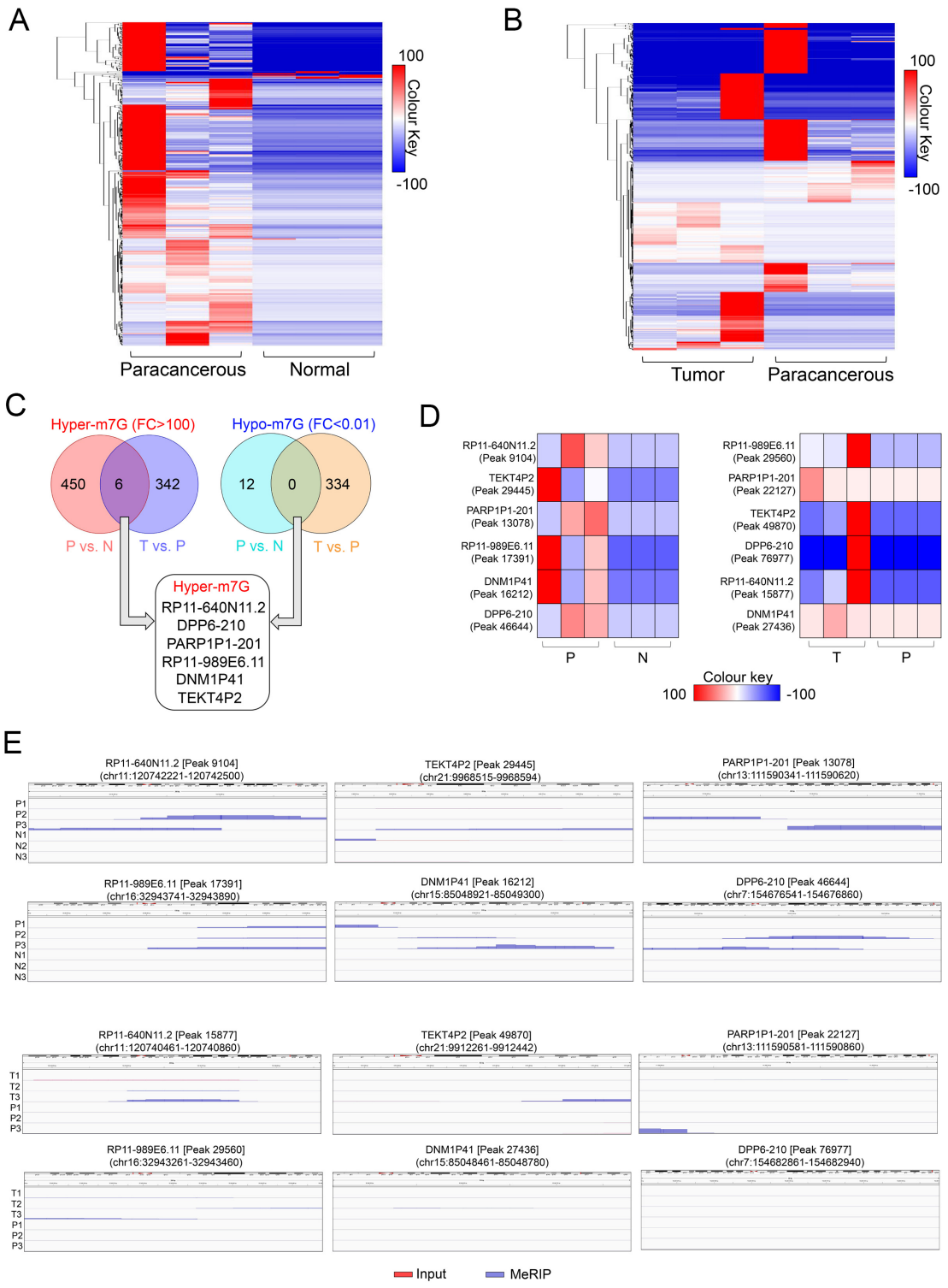

Fig. 6. Selection of lncRNAs with dynamically changing m7G modification. Heatmaps summarizing m7G alterations of peaks (FC >100 or FC <0.01) in the comparison (A) between the paracancerous tissue and the normal tissue and (B) between the HCC tissue and the paracancerous tissue. (C) Venn diagram illustrating the intersection of lncRNAs with significant m7G changes (FC >100 or FC <0.01) across different intergroup comparisons. (D) Heatmap showing the occurrence of m7G alterations across the 6 screened lncRNAs across different intergroup comparisons. (E) Visualization of the peak regions with m7G alterations in comparison between the paracancerous tissue and normal tissue (upper 6 panels) and between the HCC tissue and paracancerous tissue (lower 6 panels). MeRIP and Input were overlaid in the same track. N, normal; P, paracancerous; T, tumor; FC, fold change.

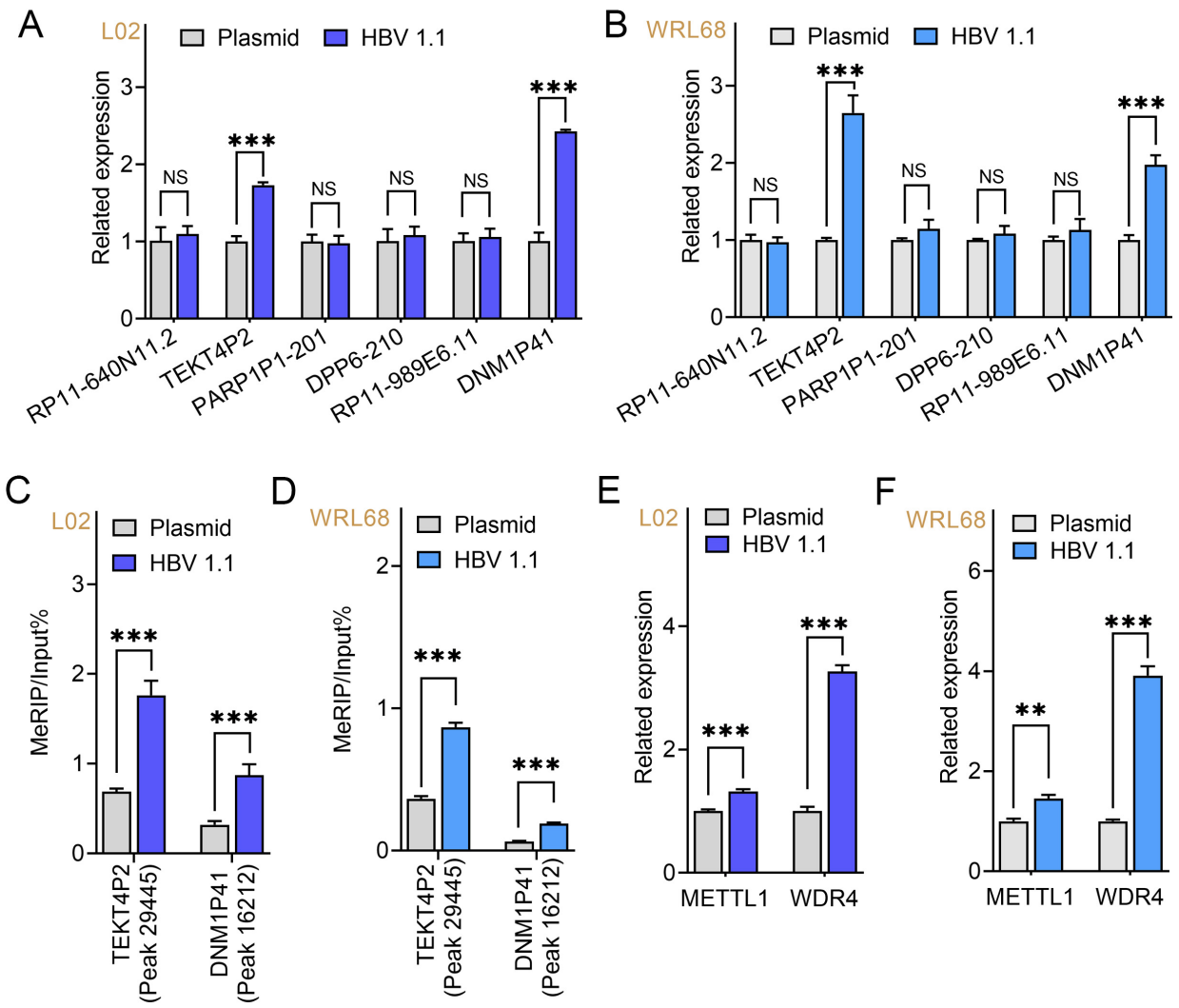

Fig. 7. Preliminary validation of identified m7G-related lncRNAs. qRT-PCR was performed to assess expression of the 6 screened potential m7G-related lncRNAs in (A) L02 cells and (B) WRL68 cells following transfection with the HBV 1.1 plasmid. Using (C) L02 cells and (D) WRL68 cells, MeRIP-PCR was carried out to examine changes in m7G levels of TEKT4P2 and DNM1P41 after HBV transfection. Levels of the m7G methyltransferases METTL1 and WDR4 were assessed by qRT-PCR in (E) L02 cells and (F) WRL68 cells following HBV transfection. The mean and SD from three independent experiments are depicted. $^{**}p < 0.01$, $^{***}p < 0.001$.

observation suggests that HBV may be involved in induction of hyper-m7G modification, which is subsequently enhanced during the process of tumorigenesis. Consequently, the overall m7G levels of relevant lncRNAs consistently increased, emphasizing the crucial role of m7G modification in the HBV-mediated inflammation-to-cancer transformation process.

Our meticulous screening process led to identification of 6 novel lncRNAs that exhibited dynamic and sustained increases in m7G levels throughout the aforementioned process. Unexpectedly, among the six screened lncRNAs, only two (TEKT4P2 and DNM1P41) were found to be regulated by HBV in terms of their expression. Despite rigorous enforcement of stringent exclusion criteria, the primary limitation of this study is the small sample size. This limitation potentially influences the obtained results to some extent, necessitating validation of screened lncRNAs in expansive clinical cohorts. Additionally, as m7G acts as an epigenetic modification, it may not dynamically influence expression of all lncRNAs, and these effects may also be counteracted by other influencing factors. Thus, we identified only TEKT4P2 and DNM1P41 as being positively regulated by HBV. Subsequent *in vitro* experimentation confirmed that TEKT4P2 and DNM1P41 are upregulated through internal m7G methylation mediated by the methyltransferase METTL1 and the associated factor WDR4. Upregulation of METTL1 has been found to promote progression of HCC [28], and further studies have revealed its ability to promote hepatocarcinogenesis by modifying m7G levels of tRNAs [29]. WDR4, as a key component of the m7G methyltransferase, is also upregulated in HCC tissues and contributes to sorafenib and lenvatinib resistance [30,31]. While the

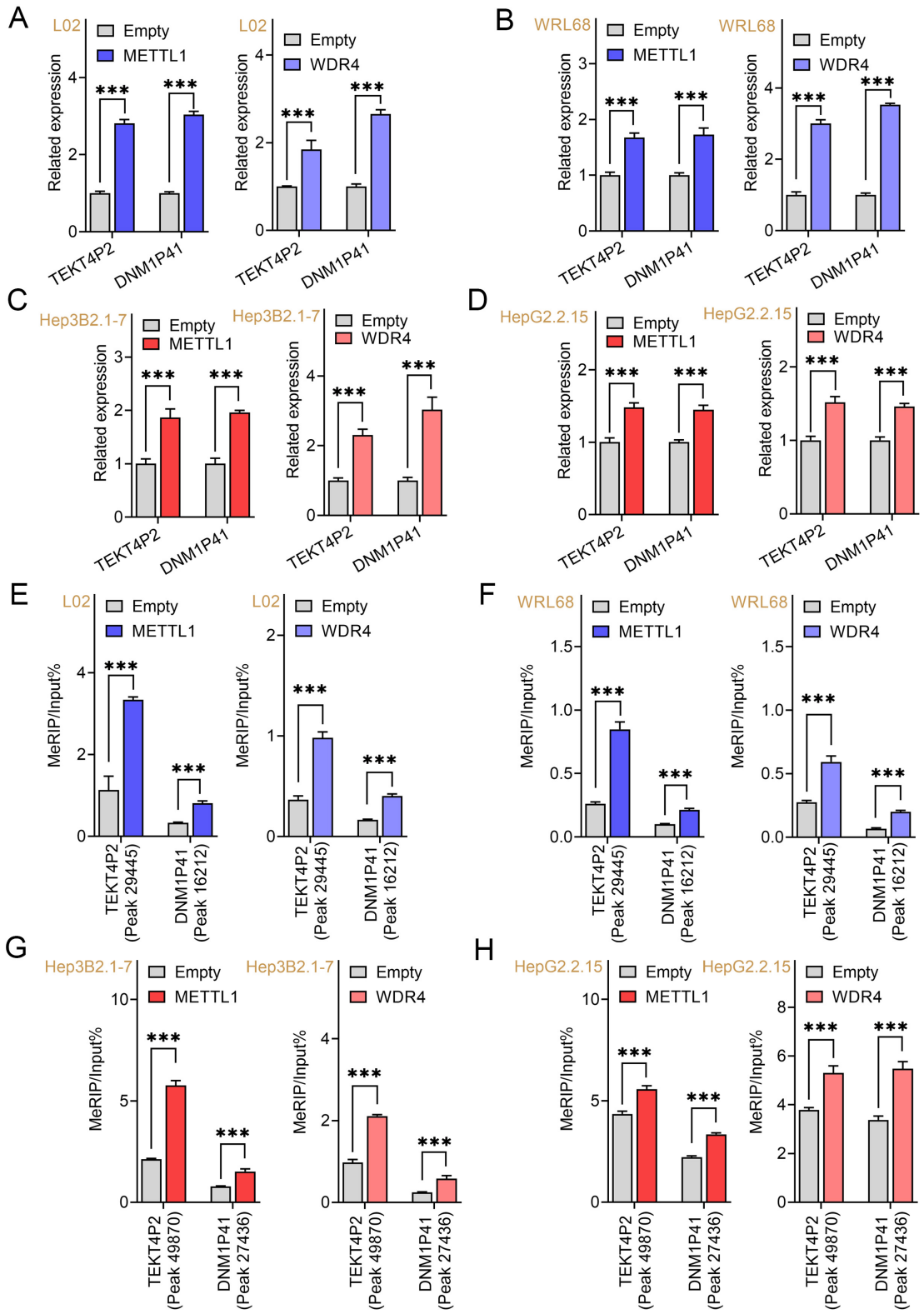

Fig. 8. The expression pattern of m7G modification-dependent dynamic lncRNAs. Expression of TEKT4P2 and DNM1P41 was assessed by qRT–PCR in normal hepatocytes (A) L02 cells and (B) WRL68 cells and hepatoma (C) Hep3B2.1-7 cells and (D) HepG2.2.15 cells after transfection of METTL1 and WDR4. MeRIP-PCR was carried out to detect m7G alteration of TEKT4P2 and DNM1P41 in (E) L02 cells, (F) WRL68 cells, (G) Hep3B2.1-7 cells, and (H) HepG2.2.15 cells following overexpression of METTL1 and WDR4. ***$p < 0.001$.

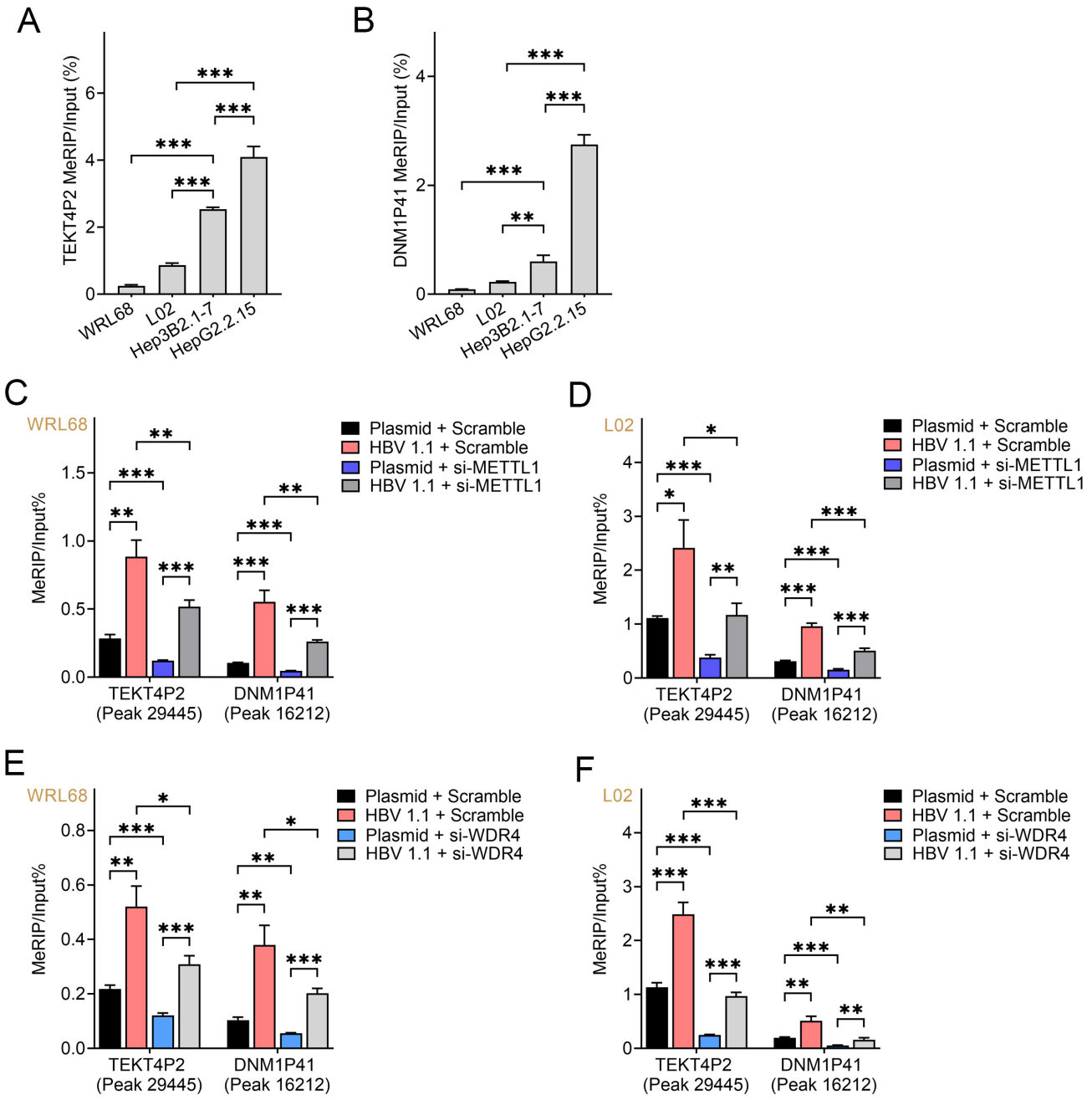

Fig. 9. The impact of HBV and methyltransferase on m7G modification of dynamic lncRNAs. m7G levels of (A) TEKT4P2 and (B) DNM1P41 in hepatocytes and hepatoma cells were determined by MeRIP-PCR. MeRIP-PCR was performed to detect changes in m7G modification of TEKT4P2 and DNM1P41 after HBV transfection and METTL1 knockdown in (C) WRL68 cells and (D) L02 cells. Alteration of m7G levels of TEKT4P2 and DNM1P41 was assessed by MeRIP-PCR following transfection of HBV and knockdown of WDR4 in (E) WRL68 cells and (F) L02 cells. *$p < 0.05$, **$p < 0.01$, ***$p < 0.001$.

regulatory mechanisms of METTL1 and WDR4 by HBV have yet to be elucidated, our study provides evidence of HBV-mediated upregulation of METTL1 and WDR4 expression. This finding aligns with a report of increased expression of METTL1 and WDR4 in HBV-infected tissues, which is the only study investigating m7G modification in chronic HBV infection [32]. In that study, the investigators clarified the relationship between m7G-related genes in HBV-infected liver tissues and the immune microenvironment as well as disease progression. They found significant upregulation of METTL1 and WDR4 in HBV-infected tissue. Furthermore, these m7G-related genes not only regulate the immune microenvironment to control hepatitis progression but also serve as potential molecular markers in this context. Hence, we propose that HBV infection upregulates expression of methyltransferases to regulate the

m7G modification of lncRNAs. During the HCC stage, further upregulation of METTL1 and WDR4 occurs, leading to increases in the internal m7G levels of specific lncRNAs. Consequently, synchronized upregulation in m7G levels and expression of TEKT4P2 and DNM1P41 renders them potential critical molecular markers for HBV-induced inflammation-to-cancer transformation, potentially participating in HBV-induced HCC formation and progression.

It is noteworthy that when summarizing intergroup differences in m7G modifications of lncRNAs, we observed a decreasing number of differentially modified lncRNAs with increasing lncRNA length. In other words, shorter lncRNAs appeared to be more susceptible to internal m7G modification. This may be because shorter lncRNAs have fewer potential binding sites for interactions with other intracellular molecules, thereby amplifying the impact of a single m7G modification peak on the overall stability or expression regulation of the RNA. On the other hand, longer lncRNAs may have reduced influence from such epigenetic modifications due to the prevalence of other regulatory mechanisms. Moreover, through utilization of GO and KEGG analyses on lncRNA transcript origins or associated genes, we observed enrichment of the Notch pathway, potentially indicating an association between HBV-mediated m7G modifications in lncRNAs and the Notch pathway. Previous studies have demonstrated the relevance of the Notch pathway in HBV replication activation, a process intricately linked to HCC progression [33,34]. Therefore, our findings suggest a potential connection between HBV regulation of the Notch pathway and internal m7G modification of key genes, providing a new theoretical framework for understanding HBV replication and its contribution to HCC formation.

Previous studies have investigated the association between m7G-related lncRNA expression and prognosis in HCC [35,36]. Additionally, research has explored the expression profiles of m7G-related lncRNAs potentially linked to immune responses and their prognostic implications in HCC [37,38]. However, there is currently a lack of work specifically examining m7G-related lncRNAs in HBV-associated HCC. Furthermore, the continuous dynamic changes in m7G-related lncRNAs throughout different stages of disease progression remain poorly understood. In our study, we thoroughly characterized and summarized the m7G methylation patterns within lncRNAs following HBV infection and hepatocarcinogenesis. We also made the novel discovery that HBV may regulate the m7G methylation patterns of lncRNAs through upregulation of METTL1 and WDR4. Through this regulatory mechanism, TEKT4P2 and DNM1P41 may serve as promising molecular markers for HBV-related inflammation-to-cancer transformation. For noncoding RNAs, internal m7G modification may affect their expression and function. In tRNA, internal hyper-m7G may increase stability [26], thereby increasing expression of m7G-related tRNAs [39]. In miRNA, internal hype-rm7G may facilitate dicer activity and maturation, thereby increasing expression [25]. However, there are currently no reports on the molecular mechanisms underlying the impact of internal m7G modification on the expression and function of lncRNAs. Our current study demonstrates that the 2 screened lncRNAs exhibit hyper-m7G and sustained upregulation during the HBV-mediated inflammation-to-cancer transition. Thus, we infer that m7G modification of TEKT4P2 and DNM1P41 plays an important role in HBV progression and ultimately induces HCC occurrence. Although the biological functions and specific molecular mechanisms of TEKT4P2 and DNM1P41 are not yet clear, our research provides valuable avenues for further exploration and investigation in our future studies.

5. Conclusions

In summary, our study compiled the methylome profiles of internal m7G modification of lncRNAs following HBV infection and the occurrence of HCC. Our results demonstrate a continuous variation in m7G levels in the process of HBV infection leading to hepatocarcinogenesis, potentially associated with HBV-mediated regulation of the m7G methyltransferases METTL1 and WDR4. Furthermore, we identified TEKT4P2 and DNM1P41 as potential molecular markers for HBV-induced inflammation-to-cancer transformation in HCC. These findings provide a novel theoretical basis for future research in this field.

Abbreviations

HCC, hepatocellular carcinoma; m7G, N7-methylguanosine; lncRNA, long non-coding RNAs; HBV, hepatitis B virus; MeRIP, methylated RNA immunoprecipitation; HHE, hepatic hemangioma; ELISA, enzyme linked immunosorbent assay; FC, fold change; qRT-PCR, quantitative reverse transcription-PCR; GEO, Gene Expression Omnibus; GO, Gene Ontology; KEGG, Kyoto Encyclopedia of Genes and Genomes; METTL1, methyltransferase 1; WDR4, WD repeat domain 4; SD, standard deviation; PARP1P1, poly(ADP-ribose) polymerase 1 pseudogene 1; DPP6, dipeptidyl peptidase like 6; TEKT4P2, tektin 4 pseudogene 2; DNM1P41, dynamin 1 pseudogene 41.

Availability of Data and Materials

The complete RNA-seq data were uploaded to the Gene Expression Omnibus (GSE237003, https://www.ncbi.nlm.nih.gov/geo/). The token key can be obtained from the corresponding author with justifications.

Author Contributions

TG, DX and SZ performed study concept and design; MS, SZ, LS, JH, NS, ML and YW performed experiments and data analyses; HL and WD obtained clinical data and

screened subjects; MS, SZ, LS, JH, YW, HL and WD provided acquisition, analysis and interpretation of data, and statistical analysis; MS, LS, JH, WD, YW and DX provided technical and material support; TG and DX writing the paper. All authors contributed to editorial changes in the manuscript. All authors read and approved the final paper. All authors have participated sufficiently in the work to take public responsibility for appropriate portions of the content and agreed to be accountable for all aspects of the work in ensuring that questions related to its accuracy or integrity.

Ethics Approval and Consent to Participate

Anonymous clinical sample collection and data analysis were authorized by the Ethics Committee of Weifang Medical University (Ref. 2021YX012), and all included patients provided signed informed consent.

Acknowledgment

Not applicable.

Funding

This study was supported by Natural Science Foundation of Shandong Province (Grant numbers: ZR2021QH200), Project of Shandong Province Youth Innovation Team (Grant numbers: 2022KJ267) and Research Start-up Funds of Weifang Medical University (Grant numbers: 04102001).

Conflict of Interest

The authors declare no conflict of interest.

Supplementary Material

Supplementary material associated with this article can be found, in the online version, at https://doi.org/10.31083/j.fbl2812339.

References

[1] Sung H, Ferlay J, Siegel RL, Laversanne M, Soerjomataram I, Jemal A, *et al*. Global Cancer Statistics 2020: GLOBOCAN Estimates of Incidence and Mortality Worldwide for 36 Cancers in 185 Countries. CA: A Cancer Journal for Clinicians. 2021; 71: 209–249.

[2] Petrick JL, Florio AA, Znaor A, Ruggieri D, Laversanne M, Alvarez CS, *et al*. International trends in hepatocellular carcinoma incidence, 1978-2012. International Journal of Cancer. 2020; 147: 317–330.

[3] Chidambaranathan-Reghupaty S, Fisher PB, Sarkar D. Hepatocellular carcinoma (HCC): Epidemiology, etiology and molecular classification. Advances in Cancer Research. 2021; 149: 1–61.

[4] Forner A, Reig M, Bruix J. Hepatocellular carcinoma. Lancet. 2018; 391: 1301–1314.

[5] Sung WK, Zheng H, Li S, Chen R, Liu X, Li Y, *et al*. Genome-wide survey of recurrent HBV integration in hepatocellular carcinoma. Nature Genetics. 2012; 44: 765–769.

[6] Jia L, Gao Y, He Y, Hooper JD, Yang P. HBV induced hepatocellular carcinoma and related potential immunotherapy. Pharmacological Research. 2020; 159: 104992.

[7] Seeger C, Mason WS. Molecular biology of hepatitis B virus infection. Virology. 2015; 479-480: 672–686.

[8] Yuen MF, Chen DS, Dusheiko GM, Janssen HLA, Lau DTY, Locarnini SA, *et al*. Hepatitis B virus infection. Nature Reviews. Disease Primers. 2018; 4: 18035.

[9] Levrero M, Zucman-Rossi J. Mechanisms of HBV-induced hepatocellular carcinoma. Journal of Hepatology. 2016; 64: S84–S101.

[10] Guerrieri F, Belloni L, Pediconi N, Levrero M. Molecular mechanisms of HBV-associated hepatocarcinogenesis. Seminars in Liver Disease. 2013; 33: 147–156.

[11] Ge WJ, Huang H, Wang T, Zeng WH, Guo M, Ren CR, *et al*. Long non-coding RNAs in hepatocellular carcinoma. Pathology, Research and Practice. 2023; 248: 154604.

[12] Zhu WP, He XG, Zhu HX, Wang LR, Lin ZH, Wang M, *et al*. Identification of miRNAs, mRNAs, lncRNAs, and circRNAs associated with hepatocellular carcinoma recurrence after interferon treatment. Journal of Biological Regulators and Homeostatic Agents. 2021; 35: 1217–1229.

[13] Zhang H, Chen X, Zhang J, Wang X, Chen H, Liu L, *et al*. Long non coding RNAs in HBV related hepatocellular carcinoma (Review). International Journal of Oncology. 2020; 56: 18–32.

[14] Wang X, Kang M, Liu C, Lin T, Han X, Jiang X. Current State and Progress of Research on the Role of lncRNA in HBV-Related Liver Cancer. Frontiers in Cellular and Infection Microbiology. 2021; 11: 714895.

[15] Zhang W, Wu W, Meng Q, Yang L, Yuan J, Tian Z, *et al*. Research Progress on Long Noncoding RNAs and N6-Methyladenosine in Hepatocellular Carcinoma. Frontiers in Oncology. 2022; 12: 907399.

[16] Luo Y, Yao Y, Wu P, Zi X, Sun N, He J. The potential role of N^7-methylguanosine (m7G) in cancer. Journal of Hematology & Oncology. 2022; 15: 63.

[17] Nassal M. The arginine-rich domain of the hepatitis B virus core protein is required for pregenome encapsidation and productive viral positive-strand DNA synthesis but not for virus assembly. Journal of Virology. 1992; 66: 4107–4116.

[18] Zhang Y, Liu T, Meyer CA, Eeckhoute J, Johnson DS, Bernstein BE, *et al*. Model-based analysis of ChIP-Seq (MACS). Genome Biology. 2008; 9: R137.

[19] Shen L, Shao NY, Liu X, Maze I, Feng J, Nestler EJ. diffReps: detecting differential chromatin modification sites from ChIP-seq data with biological replicates. PLoS ONE. 2013; 8: e65598.

[20] Thorvaldsdóttir H, Robinson JT, Mesirov JP. Integrative Genomics Viewer (IGV): high-performance genomics data visualization and exploration. Briefings in Bioinformatics. 2013; 14: 178–192.

[21] Bailey TL. DREME: motif discovery in transcription factor ChIP-seq data. Bioinformatics. 2011; 27: 1653–1659.

[22] Zhang Z, Park E, Lin L, Xing Y. A panoramic view of RNA modifications: exploring new frontiers. Genome Biology. 2018; 19: 11.

[23] Jühling F, Mörl M, Hartmann RK, Sprinzl M, Stadler PF, Pütz J. tRNAdb 2009: compilation of tRNA sequences and tRNA genes. Nucleic Acids Research. 2009; 37: D159–D162.

[24] Monecke T, Dickmanns A, Ficner R. Structural basis for m7G-cap hypermethylation of small nuclear, small nucleolar and telomerase RNA by the dimethyltransferase TGS1. Nucleic Acids Research. 2009; 37: 3865–3877.

[25] Pandolfini L, Barbieri I, Bannister AJ, Hendrick A, Andrews B, Webster N, *et al*. METTL1 Promotes let-7 MicroRNA Processing via m7G Methylation. Molecular Cell. 2019; 74: 1278–1290.e9.

[26] Orellana EA, Liu Q, Yankova E, Pirouz M, De Braekeleer E,

Zhang W, *et al*. METTL1-mediated m^7G modification of Arg-TCT tRNA drives oncogenic transformation. Molecular Cell. 2021; 81: 3323–3338.e14.
[27] Liu Y, Yang C, Zhao Y, Chi Q, Wang Z, Sun B. Overexpressed methyltransferase-like 1 (METTL1) increased chemosensitivity of colon cancer cells to cisplatin by regulating miR-149-3p/S100A4/p53 axis. Aging. 2019; 11: 12328–12344.
[28] Tian QH, Zhang MF, Zeng JS, Luo RG, Wen Y, Chen J, *et al*. METTL1 overexpression is correlated with poor prognosis and promotes hepatocellular carcinoma via PTEN. Journal of Molecular Medicine. 2019; 97: 1535–1545.
[29] Chen Z, Zhu W, Zhu S, Sun K, Liao J, Liu H, *et al*. METTL1 promotes hepatocarcinogenesis via m^7 G tRNA modification-dependent translation control. Clinical and Translational Medicine. 2021; 11: e661.
[30] Xia P, Zhang H, Xu K, Jiang X, Gao M, Wang G, *et al*. MYC-targeted WDR4 promotes proliferation, metastasis, and sorafenib resistance by inducing CCNB1 translation in hepatocellular carcinoma. Cell Death & Disease. 2021; 12: 691.
[31] Han WY, Wang J, Zhao J, Zheng YM, Chai XQ, Gao C, *et al*. WDR4/TRIM28 is a novel molecular target linked to lenvatinib resistance that helps retain the stem characteristics in hepatocellular carcinomas. Cancer Letters. 2023; 568: 216259.
[32] Zhang R, Xia Y, Dong J, Ju X, Zhou K, Cao X, *et al*. Comprehensive Analysis of m7G-Related Genes and Chronic Hepatitis B: Diagnostic Markers, Immune Microenvironment Regulation, Disease Progression. Journal of Immunology Research. 2023; 2023: 9471520.
[33] Wang Z, Kawaguchi K, Honda M, Hashimoto S, Shirasaki T, Okada H, *et al*. Notch signaling facilitates hepatitis B virus covalently closed circular DNA transcription via cAMP response element-binding protein with E3 ubiquitin ligase-modulation. Scientific Reports. 2019; 9: 1621.
[34] Gao J, Xiong Y, Wang Y, Wang Y, Zheng G, Xu H. Hepatitis B virus X protein activates Notch signaling by its effects on Notch1 and Notch4 in human hepatocellular carcinoma. International Journal of Oncology. 2016; 48: 329–337.
[35] Yang C, Zhang L, Hao X, Tang M, Zhou B, Hou J. Identification of a Novel N7-Methylguanosine-Related LncRNA Signature Predicts the Prognosis of Hepatocellular Carcinoma and Experiment Verification. Current Oncology. 2022; 30: 430–448.
[36] Li Y, Zhao K, Wu R, Wang J, Wang Q, Xiong Q, *et al*. Identification of N7-methylguanosine-related lncRNAs for the risk stratification of hepatocellular carcinoma. Journal of Gastrointestinal Oncology. 2023; 14: 1392–1411.
[37] Wang T, Zhou Z, Wang X, You L, Li W, Zheng C, *et al*. Comprehensive analysis of nine m7G-related lncRNAs as prognosis factors in tumor immune microenvironment of hepatocellular carcinoma and experimental validation. Frontiers in Genetics. 2022; 13: 929035.
[38] Dai YY, Gao YP, Chen LX, Liu JS, Zeng C, Zhou JD, *et al*. Predicting prognosis and immune responses in hepatocellular carcinoma based on N7-methylguanosine-related long noncoding RNAs. Frontiers in Genetics. 2022; 13: 930446.
[39] Han H, Yang C, Ma J, Zhang S, Zheng S, Ling R, *et al*. N^7-methylguanosine tRNA modification promotes esophageal squamous cell carcinoma tumorigenesis via the RPTOR/ULK1/autophagy axis. Nature Communications. 2022; 13: 1478.